Biomaterials Translational

Effect of radiation sterilisation on the structure and antibacterial properties of antimicrobial peptides

Xiaodan Wang[1,2,*], *Qinmei Li*[1], *Huawei Yang*[2,3,*]

Key Words:
antibacterial activity; antimicrobial peptides; radiation sterilisation

From the Contents

ABSTRACT

Antimicrobial peptides (AMPs) have recently been exploited to fabricate anti-infective medical devices due to their biocompatibility and ability to combat multidrug-resistant bacteria. Modern medical devices should be thoroughly sterilised before use to avoid cross-infection and disease transmission, consequently it is essential to evaluate whether AMPs withstand the sterilisation process or not. In this study, the effect of radiation sterilisation on the structure and properties of AMPs was explored. Fourteen AMPs formed from different monomers with different topologies were synthesised by ring-opening polymerisation of N-carboxyanhydrides. The results of solubility testing showed that the star-shaped AMPs changed from water-soluble to water-insoluble after irradiation, while the solubility of linear AMPs remained unchanged. Matrix-assisted laser desorption/ionisation time of flight mass spectrometry showed that the molecular weight of the linear AMPs underwent minimal changes after irradiation. The results of minimum inhibitory concentration assay also illustrated that radiation sterilisation had little effect on the antibacterial properties of the linear AMPs. Therefore, radiation sterilisation may be a feasible method for the sterilisation of AMPs, which have promising commercial applications in medical devices.

***Corresponding authors:**
Xiaodan Wang,
wxd@hygeamed.com;
Huawei Yang,
yanghw@ciac.ac.cn.

http://doi.org/10.12336/biomatertransl.2023.01.007

How to cite this article:
Wang, X.; Li, Q.; Yang, H. Effect of radiation sterilisation on the structure and antibacterial properties of antimicrobial peptides. *Biomater Transl.* **2023**, *4*(1), 51-61.

Introduction

Surfaces of indwelling medical devices, such as central venous catheters, prostheses and contact lenses, often suffer from microbial contamination, which ultimately leads to medical device-related infections and high risk to human health.[1-3] Therefore, extensive efforts have been made to develop effective, safe, and durable antimicrobial medical devices. In the clinical setting, antiseptic drug loading has been proven to be the most achievable method to create an antimicrobial surface on a medical device.[4-6] Silver ion-,[7,8] silver alloy-,[9,10] chlorhexidine-,[11-13] and antibiotic-impregnated central venous catheters[4,14] and urinary catheters have been widely used in hospitals and show lower risk of catheter-related infections. However, each approach possesses inherent limitations of overall poor biocompatibility and significant risks of drug resistance that will render it unsuitable for a specific product.[15,16]

Recently, antimicrobial peptides (AMPs) have attracted considerable attention for the development of antimicrobial medical devices by virtue of their broad-spectrum, rapid-acting antibacterial activity, excellent biocompatibility,[17-19] and less susceptibility to bacterial resistance evolution.[20-22] However, natural AMPs are not preferred for anti-infective medical devices due to their high-cost, unclear toxicology, and low immature stability.[17] Consequently synthetic AMPs which are less expensive and easier to prepare have been developed as good substitutes

for natural AMPs. Especially, AMPs prepared by ring-opening polymerisation (ROP) of *N*-carboxyanhydrides (NCAs) have tunable structures and properties that can be adjusted according to actual demands.[18, 23] In addition, surface-immobilised AMPs not only have high antimicrobial activity, but also exhibit much lower cytolytic potency towards mammalian cells.[24]

Sterilisation has been defined as any process that eliminates microorganisms from a surface, food, medication, or biological culture medium.[25] For medical devices, sterilisation has been recognised as an essential process.[26] Patients may suffer infection and mortality/morbidity issues when using improperly sterilised healthcare products.[26] Therefore, the AMPs loaded onto medical devices must be able to withstand the sterilisation process. Ethylene oxide gas and ionising radiation are the most widespread commercially-available non-thermal sterilisation methods for healthcare products.[27] For AMPs, amino groups are the main groups responsible for their bactericidal function.[28] Considering that an epoxy group will interact with active amino groups on the AMPs and affect their performance,[24, 29] ethylene oxide sterilisation is considered to be an unsuitable sterilisation method for AMPs, and radiation sterilisation is the preferred method. Nervetheless radiation may alter the chemical and physical properties of AMPs, to the best of our knowledge, there are no relevant studies on the validation of radiation sterilisation methods for AMPs and consequently detailed studies of potential degradation need to be performed.

In this study, fourteen AMPs consisting of different monomers and with varied topologies were synthesised through the ROP of NCAs. Validation of the AMPs against the radiation sterilisation was carried out by employing a commercial 10 MeV electron beam (e-beam). It has been reported that 25 kGy is the recommended dose for the sterilisation of medical devices with no further need to provide any biological validation.[30-34] Therefore, a radiation dose of 25 kGy was chosen for our tests. The influences of sterilisation on the structure and antibacterial properties of the AMPs were comprehensively analysed by matrix-assisted laser desorption/ionisation time of flight (MALDI-TOF) mass spectrometry (MS) and the minimum inhibitory concentration (MIC) assay.

Methods

Materials

Nε-tert-butyloxycarbonyl-L-lysine(Lys,97%),D-phenylalanine (Phe, 98%), triphosgene (99%), trifluoroacetic acid (99%), hexylamine (99%), and D, L-valine (Val, 98%) were obtained from Shanghai Aladdin Biochemical Technology Co., Ltd. (Shanghai, China). Star-shaped initiators were provided by Dendritech, Inc. (Midland, MI, USA). Sodium acetate (99.5%), dimethyl sulfoxide-d_6, chloroform-*d* were purchased from Anhui Senrise Technology Co., Ltd. (Anqing, Anhui, China). Anhydrous *N*, *N*-dimethylformamide (99.9%) and anhydrous tetrahydrofuran (99.9%) were provided by Beijing Innochem Technology Co., Ltd. (Beijing, China). Other reagents were analytically pure reagents and were used directly without treatment. *Escherichia coli* (*E. coli*, ATCC 25922) and *Staphylococcus aureus* (*S. aureus*, ATCC 6538) were purchased from Nanjing Clinic Biological Technology Co. Ltd. (Nanjing, Jiangsu, China). Bacterial culture medium and dialysis bags (molecular weight cut-offs of 3500 g/mol and 8000–12,000 g/mol) were provided by Dingguo Biological Technology Co., Ltd. (Beijing, China).

Instrumentations

^{1}H nuclear magnetic resonance spectroscopy (^{1}H-NMR) was carried out on a Bruker AV, 400 MHz spectrometer (Bruker Corporation, Billerica, MA, USA) to characterise the molecular structures of NCAs, AMPs and all intermediate products. Fourier transform infrared spectroscopy was performed on a Bruker Vertex 70 (Bruker Corporation) to ascertain the conversion rate of monomers. Gel permeation chromatography was performed on a system equipped with an isocratic pump (Model 1100, Agilent Technology, Santa Clara, CA, USA), a Dawn Heleos multi-angle laser light scattering detector (Wyatt Technology, Santa Barbara, CA, USA), and an Optilab rEX refractive index detector (Wyatt Technology). The detection wavelength of the laser light scattering detector was 658 nm. Separations were performed using serially-connected size-exclusion columns (100 Å, 500 Å, 1×10^3 Å and 1×10^4 Å Phenogel columns, 5 μm, 300 × 7.8 mm, Phenomenex Inc., Torrance, CA, USA) at 60°C using N, N-dimethylformamide containing 0.05 M LiBr as the eluent phase at a flow rate of 1.0 mL/min. MALDI-TOF MS was performed on a Bruker Daltonics FlexAnalysis system (Bruker Corporation) to measure the molecular weight of AMPs.

Preparation and characterisation of the antimicrobial peptides

In this study, fourteen AMPs consisting of different monomers and with different topological structures were synthesised by ROP of NCAs; the details are shown in **Figure 1**. ROP of NCAs is one of the most convenient methods to prepare AMPs. The specific synthetic processes of NCAs and AMPs have been reported elsewhere.[24, 35] The successful construction of all AMPs was confirmed by ^{1}H-NMR (**Additional file 1**).

Experimental process of radiation sterilisation

Each dry powdered AMP was placed in a 10 mL polypropylene tube and irradiated at room temperature at a dosage of 25 kGy by a 10 MeV e-beam accelerator at WEGO Holding Co., Ltd. (Weihai, Shandong, China) After irradiation, the samples were stored at room temperature for 5 months before characterisation. Un-irradiated samples were used as the controls to evaluate the changes caused by radiation.

1 Hygea Medical Technology Co., Ltd., Beijing, China; 2 State Key Laboratory of Polymer Physics and Chemistry, Changchun Institute of Applied Chemistry, Chinese Academy of Sciences, Changchun, Jilin Province, China; 3 Department of Applied Chemistry and Engineering, University of Science and Technology of China, Hefei, Anhui Province, China.

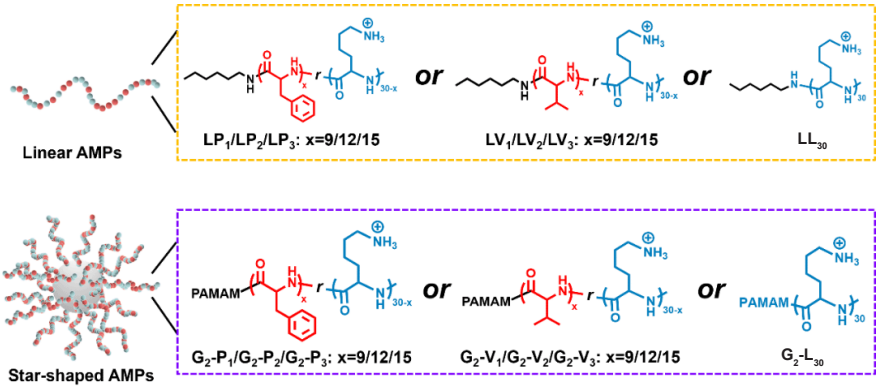

Figure 1. The molecular structure and abbreviation of each AMP in this study. AMP: antimicrobial peptide.

Evaluation of the structural changes of antimicrobial peptides

MALDI-TOF MS was used to analyse the influence of radiation sterilisation on the structure of the AMPs. Samples used for testing were prepared by dissolving in water at a concentration of 10 mg/mL.

Evaluation of the solubility of antimicrobial peptides

Approximately 10 mg of each AMP were weighed and dispersed in phosphate-buffered saline (PBS), PBS: acetic acid (v:v, 1:1) and hexafluoroisopropanol. The dissolution results were observed directly after sonication for 2 hours.

Evaluation of the antibacterial activity of antimicrobial peptides

The antibacterial activity of different AMPs before and after irradiation was determined by the MIC assay.[36, 37] The MIC of an antimicrobial agent refers to the critical concentration that inhibits bacterial growth absolutely. In this study, bacterial proliferation was analysed by measuring the optical density of the culture. *E. coli* and *S. aureus* were selected as representative Gram-negative and -positive bacteria for testing. The detailed process was as follows;[38] an overnight bacterial suspension was inoculated into Mueller-Hinton broth at 37°C with constant shaking. The bacteria were then harvested when in the logarithmic phase of growth. The bacterial density of the suspension was adjusted to 1×10^8 colony forming units (CFU)/mL, confirmed by an optical density value of 0.1 at 600 nm. Then the bacterial suspension was diluted 100 times to obtain a bacterial density of 1×10^6 CFU/mL. The AMPs were dissolved in PBS to obtain concentrations ranging from 1 μg/mL to 1000 μg/mL. Then, 100 μL of each AMP solution and 100 μL of bacterial suspension (1×10^6 CFU/mL) were added together to wells of a 96-well plate, which was then incubated at 37°C. The optical density values of the wells were measured using a microplate reader (Tecan Sunrise, Tecan Group Ltd., Männedorf, Switzerland) at 0, 6, 12, and 24 hours. A mixture of 100 μL PBS and 100 μL of bacterial solution (1×10^6 CFU/mL) was used as control.

Statistical analysis

All data are presented as mean ± standard deviation (SD). Each result is an average of at least three parallel experiments, calculated using Microsoft® Excel® 2019 (Microsoft, Redmond, WA, USA).

Results

Structural characterisation and solubility exploration of the antimicrobial peptides

First, fourteen AMPs were synthesised via ROP of three NCAs (**Figure 1**). All structures of the intermediate products and final AMPs were confirmed by ^{1}H-NMR. As shown in **Additional file 1**, the actual monomer components were consistent with the feed expectation. Combined with the results of gel permeation chromatography, the results proved that AMPs were successfully constructed. The detailed molecular parameters are shown in **Table 1**.

The solubility of AMPs before and after irradiation is shown in **Table 2**. All linear polypeptides could be dissolved in PBS regardless of irradiation, demonstrating that there was no effect of irradiation on solubility. In contrast, the star-shaped AMPs became insoluble in PBS after irradiation and only soluble in certain organic solvents, such as hexafluoroisopropanol. In order to prevent the interference of different solvents with the antibacterial properties of AMPs, linear AMPs with good solubility before and after irradiation in PBS were chosen for further investigation.

Structural changes to antimicrobial peptides caused by radiation sterilisation

Detailed information on the molecular structures and molecular weights of the monomers and AMPs is shown in **Figure 2**. The molecular weight of all AMPs ranged from 3500 to 4500, and MALDI-TOF MS was selected as a convenient instrumental method to determine the effect of radiation sterilisation on the molecular structure. (Fourier transform infrared spectroscopy and ^{1}H-NMR could not detect the tiny changes before and after sterilisation). **Figures 3–5** show the molecular weights of the linear AMPs before and after irradiation. Overall, the shapes of the MS spectrum of all samples maintained good consistency before and after irradiation. In the spectrum of the homopolymer of Lys (**Figure 3**), molecular weight intervals that corresponded to the molecular weight (128.2) of Lys monomer appeared, besides the peaks representative of $[M+H]^+$, $[M+Na]^+$, and $[M+K]^+$. Similarly, in the AMPs that copolymerised with Phe and Lys (**Figure 4**), a series of

Table 1. Detailed molecular parameters of the antimicrobial peptides

Sample	Arm No.	Designed Lys content (%)	Actual Lys content[a] (%)	Mn designed molecular weight (Da)	Mn determined molecular weight (Da)[b]	*Đ* determined molecular weight[b]
LP_1	1	70	70.8	6219.9	6200	1.07
LP_2	1	60	61.4	5976.6	6000	1.14
LP_3	1	50	51.2	5733.2	5700	1.24
G_2-P_1	16	70	71	101155.6	111200	1.05
G_2-P_2	16	60	60	97262.3	97300	1.08
G_2-P_3	16	50	48.2	93369	93400	1.12
LV_1	1	70	68.6	5787.5	5800	1.11
LV_2	1	60	59.3	5400	5500	1.09
LV_3	1	50	49	5012.5	5000	1.18
G_2-V_1	16	70	72.3	94236.4	94300	1.02
G_2-V_2	16	60	59.1	88036.7	88000	1.07
G_2-V_3	16	50	50	81837	81900	1.14
LL_{30}	1	100	100	6949.9	6900	1.05
G_2-L_{30}	16	100	100	112835.4	113000	1.13

Note: "a" represents Lys contents calculated by ^{1}H nuclear magnetic resonance spectroscopy. "b" represents the Mn and Đ determined by gel permeation chromatography. Đ: polydispersity; Lys: L-lysine.

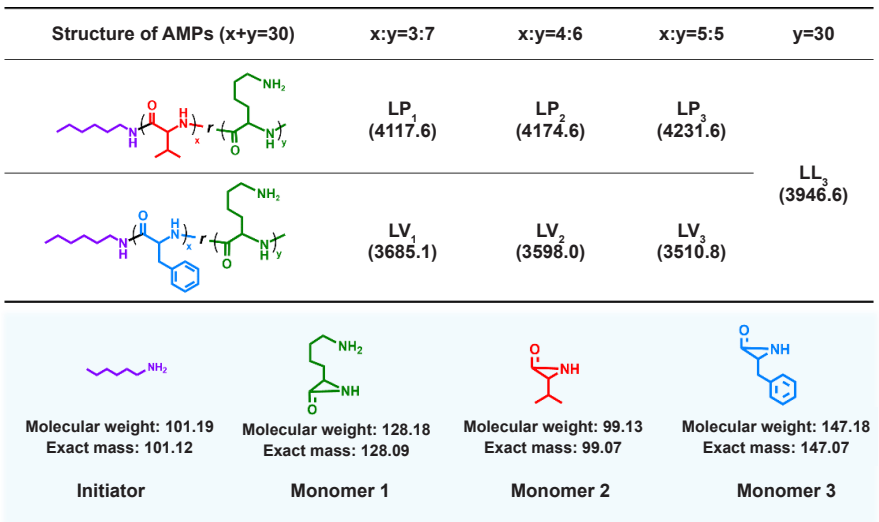

Figure 2. Molecular structure and molecular weight information of all linear AMPs. AMP: antimicrobial peptide.

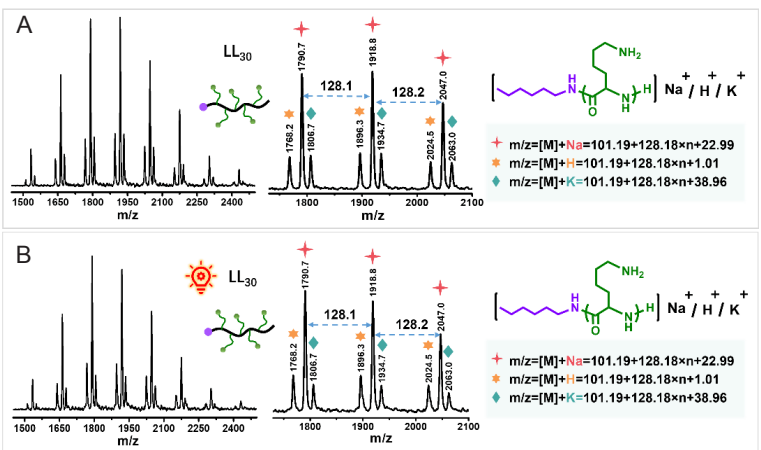

Figure 3. The spectra of LL_{30} before (A) and after (B) irradiation under matrix-assisted laser desorption/ionisation time of flight (MALDI-TOF) mass spectrometry.

Table 2. Solubility of the antimicrobial peptides before and after radiation sterilisation

	Before radiation sterilisation	After radiation sterilisation		
Sample	**PBS buffer**	**PBS buffer**	**PBS/AcOH**	**HFP**
LP_1	+	+	+	+
LP_2	+	+	+	+
LP_3	+	+	+	+
G_2-P_1	+	–	±	+
G_2-P_2	+	–	–	+
G_2-P_3	+	–	–	+
LV_1	+	+	+	+
LV_2	+	+	+	+
LV_3	+	+	+	+
G_2-V_1	+	–	–	±
G_2-V_2	+	–	–	±
G_2-V_3	+	–	–	±
LL_{30}	+	+	+	+
G_2-L_{30}	+	–	±	+

Note: "+" represents soluble, "–" represents insoluble, and "±" represents slightly soluble. AcOH: acetic acid; HFP: hexafluoroisopropanol; PBS: phosphate-buffered saline.

molecular weight intervals of 147.2, 128.2, 19.0, 109.1 and 90.2 could be seen in the spectra, which corresponded to the molecular weight of Phe monomer, Lys monomer and the molecular weight differences of Phe-Lys, 2Phe-Lys and 3Phe-2Lys (**Figures 2** and **4**). Also, for the copolymer products of Val and Lys (**Figure 5**), molecular weight intervals of 147.2, 128.2, 29.1, 70.1 and 41.0 appeared, indicating the molecular weights of Val monomer, Lys monomer, and the molecular weight differences of Lys-Val, 2Val-Lys and 3Val-2Lys (**Figures 2** and **5**).

Antibacterial performance of the antimicrobial peptides before and after irradiation

As shown in **Figures 6–8**, the antibacterial effects of all samples before and after irradiation against both Gram-positive *S. aureus* and Gram-negative *E. coli* were analysed. The MIC values are summarised in **Table 3**. The MIC of LV_2 against *S. aureus* and the MIC of LV_3 against *S. aureus* and *E. coli* increased by a factor of two after irradiation, showing a decrease in the antibacterial activity of LV_2 and LV_3. The MICs of all the other irradiated AMPs remained the same as before irradiation.

Table 3. The minimum inhibitory concentrations (μg/mL) of antimicrobial peptides against *S. aureus* and *E. coli* before and after irradiation

	S. aureus	***E. coli***
LL_{30}		
Before irradiation	16	16
After irradiation	16	16
LP_2		
Before irradiation	16	32
After irradiation	16	32
LP_2		
Before irradiation	16	32
After irradiation	16	32
LP_3		
Before irradiation	16	32
After irradiation	16	32
LV_1		
Before irradiation	16	8
After irradiation	16	8
LV_2		
Before irradiation	8	16
After irradiation	16	16
LV_3		
Before irradiation	16	32
After irradiation	32	64

Note: *E. coli*: *Escherichia coli*; *S. aureus*: *Staphylococcus aureus*.

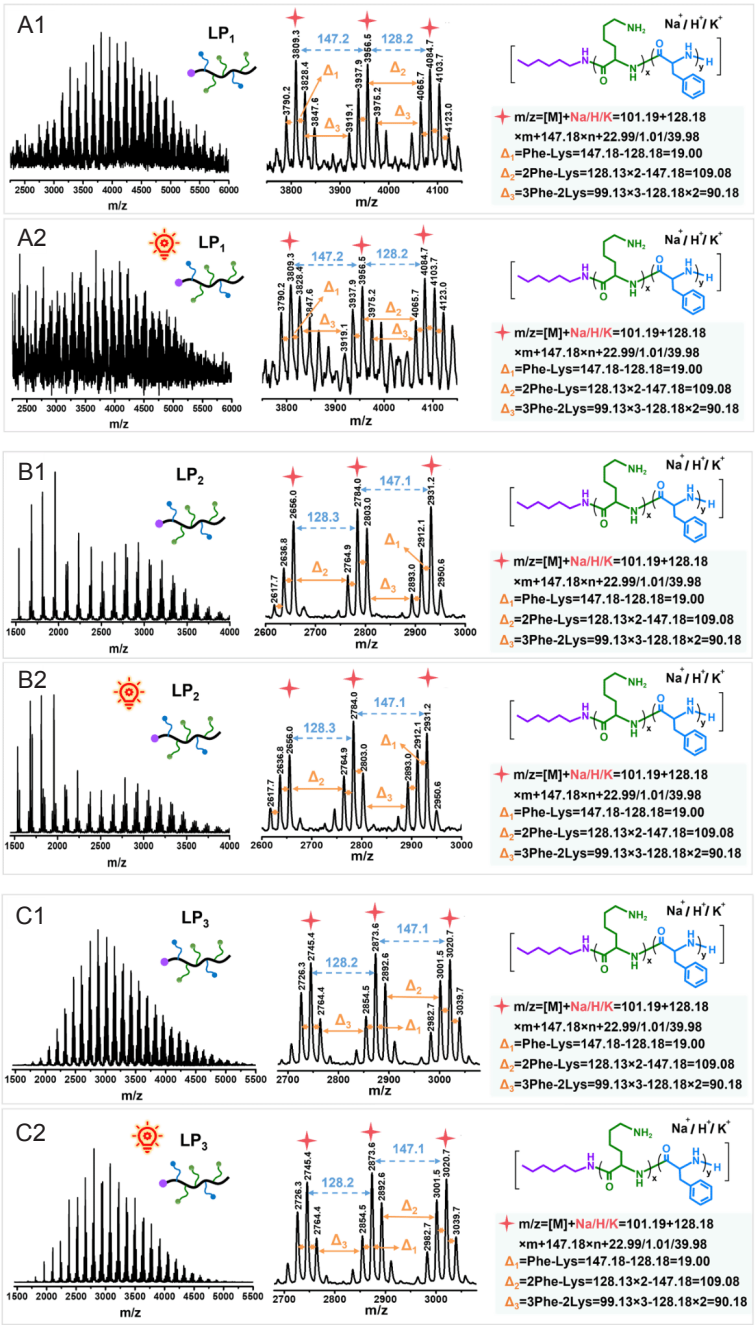

Figure 4. The spectra of LP_1–LP_3 before (A1–C1) and after (A2–C2) irradiation under matrix-assisted laser desorption/ionisation time of flight (MALDI-TOF) mass spectrometry.

Discussion

Structural changes of the antimicrobial peptides caused by radiation sterilisation

The purpose of the sterilisation process is to obtain material free from microorganisms. The ideal sterilisation process requires fully killing any pathogenic bacteria carried by a medical device. The instantaneity and high dose delivery of a high-energy e-beam allow sterilisation of products in hermetically-sealed packages. Meanwhile, the influence of radiation on the degradation of polymers is one of the most important concerns of scientific interest. Unpredictable degradation may affect their physicochemical properties, and thus affect the efficacy and safety of treatment.[32] It has been reported that ionising radiation may cause cross-linking or chain-scission.[26, 34, 39] When a cross-linking reaction occurs, the molecular weight of the polymer increases. In contrast, when the polymer undergoes a chain-scission process, the molecular weight of the polymer decreases. Therefore, the structural changes of the irradiated AMPs can be analysed by comparing the molecular weights of the corresponding AMPs before and after irradiation.

The process of radiation sterilisation had a negligible effect on the molecular weight of most AMPs. Nevertheless, careful comparison and analysis revealed a slight shift to lower

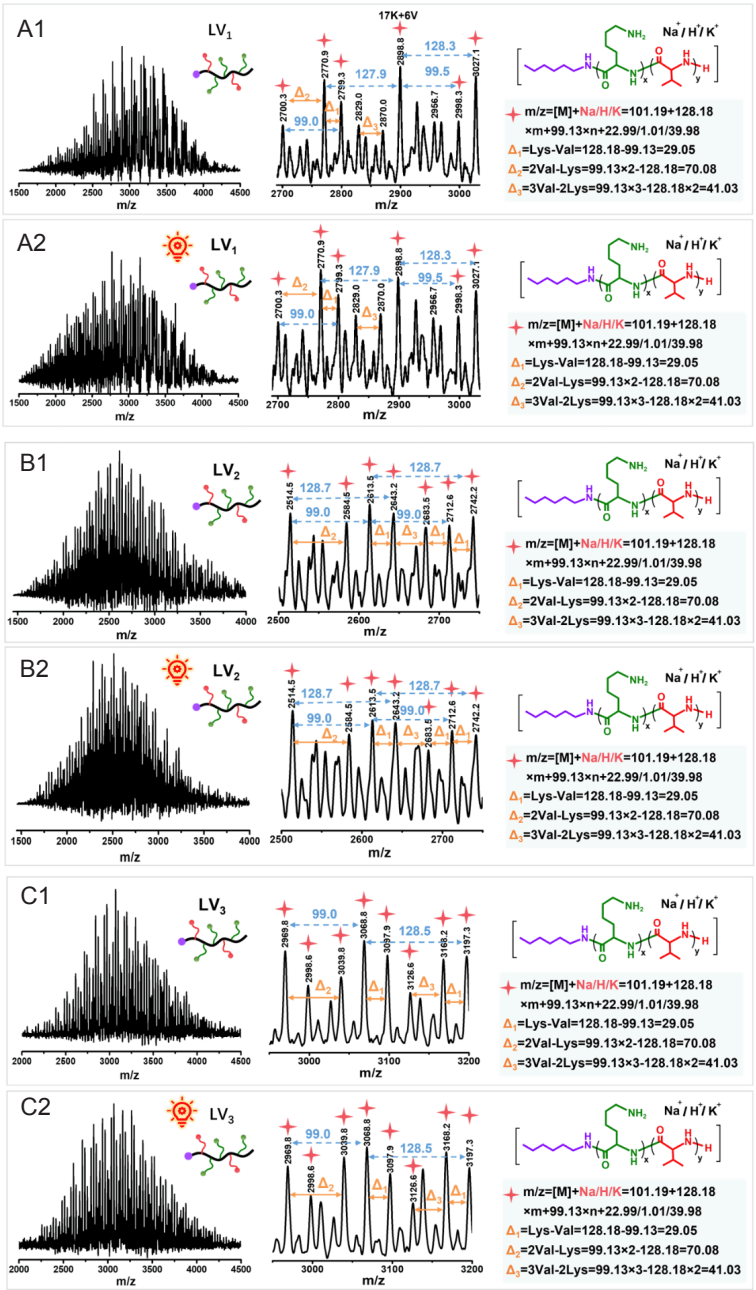

Figure 5. The spectra of LV_1–LV_3 before (A1–C1) and after (A2–C2) irradiation under matrix-assisted laser desorption/ionisation time of flight (MALDI-TOF) mass spectrometry.

molecular weight in some samples. The phenomenon was observed more obviously in the AMPs copolymerised from higher proportions of cationic Lys, regardless of whether they were copolymerised with either Phe or Val. For example, after irradiation, the molecular weight portions of LP_1 (**Figure 4A**) and LP_2 (**Figure 4B**) below 3000 g/mol were increased compared with the corresponding spectra before irradiation, indicating that molecular chains of the samples were partially broken. Similar phenomena were also observed in LV_1 (**Figure 5A**) and LV_2 (**Figure 5B**). However, the molecular weights of the samples with lower Lys, LP_3 and LV_3, showed no migration to low molecular weights. Some studies have reported that aromatic materials offer more resistance to radiation than aliphatic materials.[31] After being irradiated, the conjugated structure of aromatic rings can transfer and disperse the radiation energy by a delocalisation effect instead of concentrating on a certain bond, and as a consequence, the absorbed radiation energy will be converted into heat energy for release. Therefore, the materials generally show better radiation resistance when their main chain or side chain contains aromatic rings.[31] Accordingly, the AMPs composed of a higher proportion of Phe (LP_3) in this study showed better resistance to e-beam radiation than the AMPs with lower proportions of Phe (LP_1 and LP_2). However, these changes were tiny, and the results of MALDI-TOF MS demonstrated overall an insignificant influence of radiation sterilisation on the structure of AMPs. However, the mechanism behind the change of solubility of star-shaped AMPs was unclear.

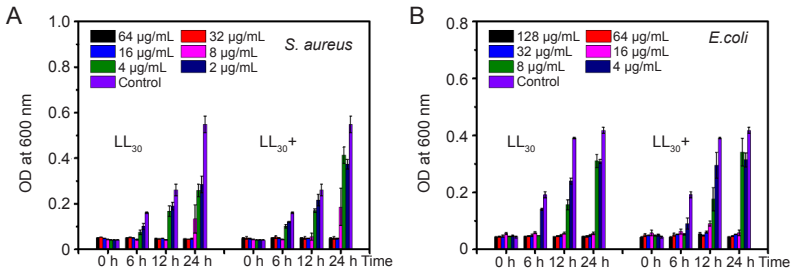

Figure 6. The minimum inhibitory concentrations of LL_{30} before and after irradiation. (A) *Staphylococcus aureus* (*S. aureus*). (B) *Escherichia coli* (*E. coli*). OD: optical density.

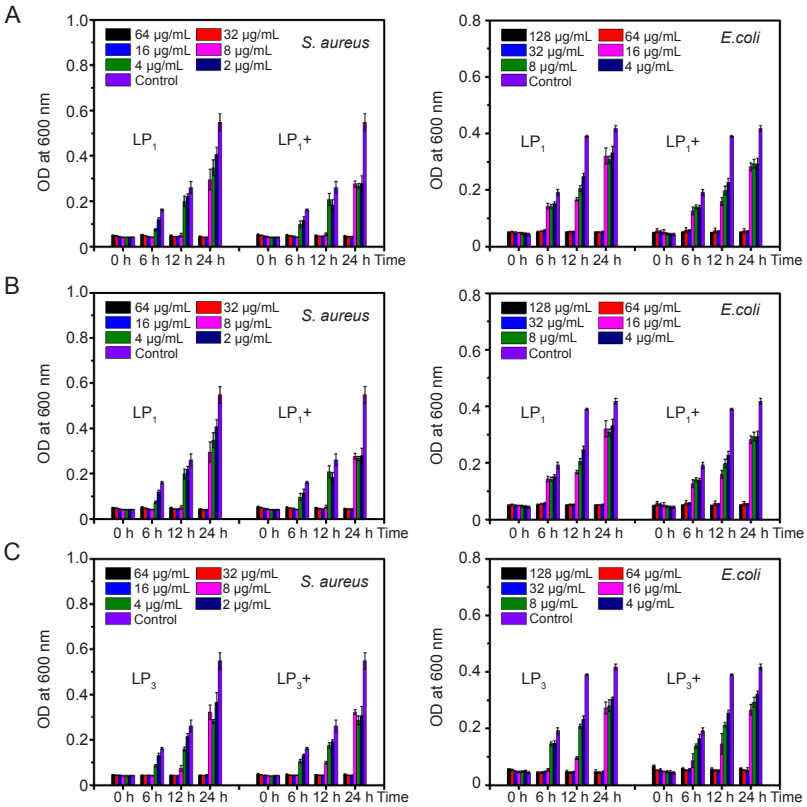

Figure 7. The minimum inhibitory concentrations of LP_1–LP_3 (A–C) before and after irradiation. *E. coli*: *Escherichia coli*; OD: optical density; *S. aureus*: *Staphylococcus aureus*.

Antibacterial property of antimicrobial peptides before and after irradiation

The antibacterial activity of AMPs is closely related to their architecture and monomer composition.[40-43] In order to explore universal laws governing the effect of radiation on the AMPs, fourteen AMPs with different architectures and varied monomer components were designed. As the star-shaped AMPs were found to be insoluble in water after radiation sterilisation, only the antibacterial properties of linear AMPs were analysed. The results of MALDI-TOF MS revealed that a high-energy e-beam caused the chain-scission of the samples. Free radicals can also be evoked in the process of chain-scission in an air atmosphere due to the presence of oxygen during the radiation process.[26, 31] Generally, decay reactions of free radicals will happen rapidly within hours to months, depending on the chemical structure of the samples, the radiation dose and the storage environment.[44-48] In order to eliminate the possible influence of free radicals, the samples were characterised at 5 months after irradiation to ensure the free radicals were fully consumed. From the results, MIC of most AMPs (except for LV_2 and LV_3) remained unchanged, indicating negligible effects of radiation on the antibacterial activity of those AMPs. Combined with the results of MALDI-TOF MS, radiation sterilisation could be considered as a feasible method to sterilise AMPs.

Conclusion

In conclusion, fourteen AMPs with different topologies (linear and star-shaped) and varied monomer components were designed and synthesised successfully. Commercial-scale 10 MeV e-beam radiation was selected as a promising sterilisation method for AMPs, and the AMPs were subjected

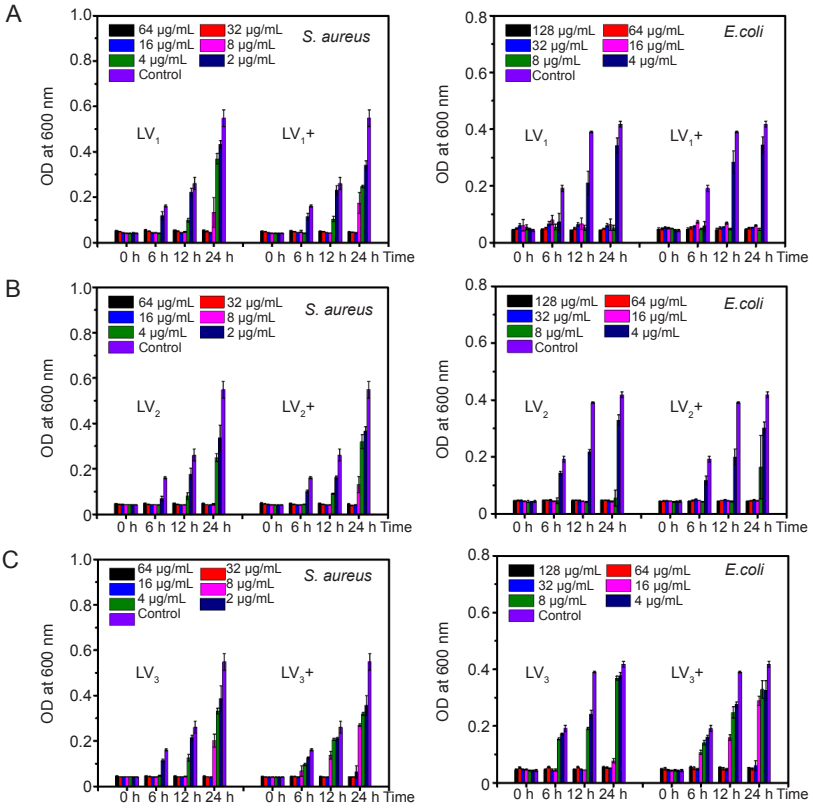

Figure 8. The minimum inhibitory concentrations of LV_1–LV_3 (A–C) before and after irradiation. *E. coli*: *Escherichia coli*; OD: optical density; *S. aureus*: *Staphylococcus aureus*.

to a dose of 25 kGy in order to explore the possible impact of radiation on their structure and antibacterial properties. It is worth mentioning that the water solubility of star-shaped AMPs changed from soluble to insoluble after irradiation. As for linear AMPs, the results of MALDI-TOF MS and MIC assay suggested negligible effects of radiation on the structure or antibacterial activity. Nevertheless, AMPs copolymerised with a higher proportion of Phe exhibited better resistance to radiation. In conclusion, radiation sterilisation is presented as an attractive and effective sterilisation strategy for AMP-based medical devices. However, there remain some problems that need further exploration. For example, characterisation of the structure and antibacterial properties of AMPs is relatively simple, but electronic paramagnetic resonance spectroscopy would be a more direct detection method for monitoring free radicals. In addition, a maximum dose that ensures the safety (biocompatibility) and performance (functionality) of the product over its lifetime also needs to be established.

Author contributions

Conceptualisation and methodology: XW, HY; investigation and resources: XW, HY, QL; formal analysis, visualisation, validation and manuscript draft: XW; manuscript revision, funding acquisition and project administration: HY; supervision: QL, HY. All authors approved the final version of the manuscript.

Financial support

None.

Acknowledgement

This study was supported by the National Natural Science Foundation of China (No. 51873213), High-Tech Research & Development Program of CAS-WEGO Group, and National Key Research and Development Program of China (No. 2021YFC2101700).

Conflicts of interest statement

There are no conflicts to declare.

Additional file

Additional file 1: Preparation and characterisation of the N-carboxyanhydrides and antimicrobial peptides.

1. Deusenbery, C.; Wang, Y.; Shukla, A. Recent innovations in bacterial infection detection and treatment. *ACS Infect Dis.* **2021**, *7*, 695-720.
2. Yu, Q.; Wu, Z.; Chen, H. Dual-function antibacterial surfaces for biomedical applications. *Acta Biomater.* **2015**, *16*, 1-13.
3. Bai, D.; Chen, J.; Li, P.; Huang, W. Perspectives on biomaterial-associated infection: pathogenesis and current clinical demands. In *Racing for the surface: pathogenesis of implant infection and advanced antimicrobial strategies*, Li, B.; Moriarty, T. F.; Webster, T.; Xing, M., eds.; Springer International Publishing: Cham, 2020; pp 75-93.
4. Lai, N. M.; Chaiyakunapruk, N.; Lai, N. A.; O'Riordan, E.; Pau, W. S.; Saint, S. Catheter impregnation, coating or bonding for reducing central venous catheter-related infections in adults. *Cochrane Database Syst Rev.* **2016**, *3*, CD007878.
5. Cloutier, M.; Mantovani, D.; Rosei, F. Antibacterial coatings: challenges, perspectives, and opportunities. *Trends Biotechnol.* **2015**, *33*, 637-652.
6. Campoccia, D.; Montanaro, L.; Arciola, C. R. A review of the biomaterials technologies for infection-resistant surfaces. *Biomaterials.*

2013, *34*, 8533-8554.

7. Chen, Y. M.; Dai, A. P.; Shi, Y.; Liu, Z. J.; Gong, M. F.; Yin, X. B. Effectiveness of silver-impregnated central venous catheters for preventing catheter-related blood stream infections: a meta-analysis. *Int J Infect Dis.* **2014**, *29*, 279-286.
8. Rupp, M. E.; Fitzgerald, T.; Marion, N.; Helget, V.; Puumala, S.; Anderson, J. R.; Fey, P. D. Effect of silver-coated urinary catheters: efficacy, cost-effectiveness, and antimicrobial resistance. *Am J Infect Control.* **2004**, *32*, 445-450.
9. Singh, R.; Hokenstad, E. D.; Wiest, S. R.; Kim-Fine, S.; Weaver, A. L.; McGree, M. E.; Klingele, C. J.; Trabuco, E. C.; Gebhart, J. B. Randomized controlled trial of silver-alloy-impregnated suprapubic catheters versus standard suprapubic catheters in assessing urinary tract infection rates in urogynecology patients. *Int Urogynecol J.* **2019**, *30*, 779-787.
10. Saint, S.; Elmore, J. G.; Sullivan, S. D.; Emerson, S. S.; Koepsell, T. D. The efficacy of silver alloy-coated urinary catheters in preventing urinary tract infection: a meta-analysis. *Am J Med.* **1998**, *105*, 236-241.
11. Safdar, N.; O'Horo, J. C.; Ghufran, A.; Bearden, A.; Didier, M. E.; Chateau, D.; Maki, D. G. Chlorhexidine-impregnated dressing for prevention of catheter-related bloodstream infection: a meta-analysis. *Crit Care Med.* **2014**, *42*, 1703-1713.
12. Lorente, L. Review: chlorhexidine-impregnated dressings reduce risk of colonisation of central venous catheters and risk of catheter-related bloodstream infection. *Evid Based Nurs.* **2015**, *18*, 91.
13. Srisang, S.; Nasongkla, N. Spray coating of foley urinary catheter by chlorhexidine-loadedpoly(ε-caprolactone) nanospheres: effect of lyoprotectants, characteristics, and antibacterial activity evaluation. *Pharm Dev Technol.* **2019**, *24*, 402-409.
14. Bayston, R.; Fisher, L. E.; Weber, K. An antimicrobial modified silicone peritoneal catheter with activity against both Gram-positive and Gram-negative bacteria. *Biomaterials.* **2009**, *30*, 3167-3173.
15. Luther, E. M.; Schmidt, M. M.; Diendorf, J.; Epple, M.; Dringen, R. Upregulation of metallothioneins after exposure of cultured primary astrocytes to silver nanoparticles. *Neurochem Res.* **2012**, *37*, 1639-1648.
16. Blair, J. M.; Webber, M. A.; Baylay, A. J.; Ogbolu, D. O.; Piddock, L. J. Molecular mechanisms of antibiotic resistance. *Nat Rev Microbiol.* **2015**, *13*, 42-51.
17. Tan, P.; Fu, H.; Ma, X. Design, optimization, and nanotechnology of antimicrobial peptides: From exploration to applications. *Nano Today.* **2021**, *39*, 101229.
18. Rasines Mazo, A.; Allison-Logan, S.; Karimi, F.; Chan, N. J.; Qiu, W.; Duan, W.; O'Brien-Simpson, N. M.; Qiao, G. G. Ring opening polymerization of α-amino acids: advances in synthesis, architecture and applications of polypeptides and their hybrids. *Chem Soc Rev.* **2020**, *49*, 4737-4834.
19. Luong, H. X.; Thanh, T. T.; Tran, T. H. Antimicrobial peptides - advances in development of therapeutic applications. *Life Sci.* **2020**, *260*, 118407.
20. Hancock, R. E.; Sahl, H. G. Antimicrobial and host-defense peptides as new anti-infective therapeutic strategies. *Nat Biotechnol.* **2006**, *24*, 1551-1557.
21. Ageitos, J. M.; Sánchez-Pérez, A.; Calo-Mata, P.; Villa, T. G. Antimicrobial peptides (AMPs): Ancient compounds that represent novel weapons in the fight against bacteria. *Biochem Pharmacol.* **2017**, *133*, 117-138.
22. Mowery, B. P.; Lee, S. E.; Kissounko, D. A.; Epand, R. F.; Epand, R. M.; Weisblum, B.; Stahl, S. S.; Gellman, S. H. Mimicry of antimicrobial host-defense peptides by random copolymers. *J Am Chem Soc.* **2007**, *129*, 15474-15476.
23. Deming, T. J. Synthesis of side-chain modified polypeptides. *Chem Rev.* **2016**, *116*, 786-808.
24. Wang, X.; Yang, F.; Yang, H.; Zhang, X.; Tang, H.; Luan, S. Preparation of antibacterial polypeptides with different topologies and their antibacterial properties. *Biomater Sci.* **2022**, *10*, 834-845.
25. Raza, S.; Iqbal, Y.; Ullah, I.; Mubarak, M. S.; Hameed, M. U.; Raza, M. Effects of gamma irradiation on the physico-chemical and biological properties of levofloxacin. *Pak J Pharm Sci.* **2018**, *31*, 181-186.
26. Gomes, A. D.; de Oliveira, A. A. R.; Houmard, M.; Nunes, E. H. M. Gamma sterilization of collagen/hydroxyapatite composites: Validation and radiation effects. *Appl Radiat Isot.* **2021**, *174*, 109758.
27. Domańska, I. M.; Oledzka, E.; Sobczak, M. Sterilization process of polyester based anticancer-drug delivery systems. *Int J Pharm.* **2020**, *587*, 119663.
28. Maturana, P.; Gonçalves, S.; Martinez, M.; Espeche, J. C.; Santos, N. C.; Semorile, L.; Maffia, P. C.; Hollmann, A. Interactions of "de novo" designed peptides with bacterial membranes: Implications in the antimicrobial activity. *Biochim Biophys Acta Biomembr.* **2020**, *1862*, 183443.
29. Yang, Z.; Xi, Y.; Bai, J.; Jiang, Z.; Wang, S.; Zhang, H.; Dai, W.; Chen, C.; Gou, Z.; Yang, G.; Gao, C. Covalent grafting of hyperbranched poly-L-lysine on Ti-based implants achieves dual functions of antibacteria and promoted osteointegration in vivo. *Biomaterials.* **2021**, *269*, 120534.
30. Bargh, S.; Silindir-Gunay, M.; Ozer, A. Y.; Colak, S.; Kutlu, B.; Nohutcu, R. The effects of gamma and microwave sterilization on periodontological grafts. *Chemical Physics Impact.* **2021**, *3*, 100046.
31. Sharma, A.; Anup, N.; Tekade, R. K. Chapter 21 - Achieving sterility in biomedical and pharmaceutical products (part-II): radiation sterilization. In *The future of pharmaceutical product development and research*, Tekade, R. K., ed. Academic Press: 2020; pp 789-848.
32. Nguyen, H.; Cassady, A. I.; Bennett, M. B.; Gineyts, E.; Wu, A.; Morgan, D. A.; Forwood, M. R. Reducing the radiation sterilization dose improves mechanical and biological quality while retaining sterility assurance levels of bone allografts. *Bone.* **2013**, *57*, 194-200.
33. De Guzman, Z. M.; Cervancia, C. R.; Dimasuay, K. G.; Tolentino, M. M.; Abrera, G. B.; Cobar, M. L.; Fajardo, A. C., Jr.; Sabino, N. G.; Manila-Fajardo, A. C.; Feliciano, C. P. Radiation inactivation of Paenibacillus larvae and sterilization of American Foul Brood (AFB) infected hives using Co-60 gamma rays. *Appl Radiat Isot.* **2011**, *69*, 1374-1379.
34. B.G. Porto, K. M.; Napolitano, C. M.; Borrely, S. I. Gamma radiation effects in packaging for sterilization of health products and their constituents paper and plastic film. *Radiat Phys Chem.* **2018**, *142*, 23-28.
35. Liu, H.; Zhang, X.; Zhao, Z.; Yang, F.; Xue, R.; Yin, L.; Song, Z.; Cheng, J.; Luan, S.; Tang, H. Efficient synthesis and excellent antimicrobial activity of star-shaped cationic polypeptides with improved biocompatibility. *Biomater Sci.* **2021**, *9*, 2721-2731.
36. Wiegand, I.; Hilpert, K.; Hancock, R. E. Agar and broth dilution methods to determine the minimal inhibitory concentration (MIC) of antimicrobial substances. *Nat Protoc.* **2008**, *3*, 163-175.
37. Li, P.; Poon, Y. F.; Li, W.; Zhu, H. Y.; Yeap, S. H.; Cao, Y.; Qi, X.; Zhou, C.; Lamrani, M.; Beuerman, R. W.; Kang, E. T.; Mu, Y.; Li, C. M.; Chang, M. W.; Leong, S. S.; Chan-Park, M. B. A polycationic antimicrobial and biocompatible hydrogel with microbe membrane suctioning ability. *Nat Mater.* **2011**, *10*, 149-156.
38. Wang, X.; Shi, H.; Tang, H.; Yu, H.; Yan, Q.; Yang, H.; Zhang, X.;

Luan, S. Electrostatic assembly functionalization of poly (γ-glutamic acid) for biomedical antibacterial applications. *J Mater Sci Technol.* **2020**, *59*, 14-25.

39. Haji-Saeid, M.; Sampa, M. H. O.; Chmielewski, A. G. Radiation treatment for sterilization of packaging materials. *Radiat Phys Chem.* **2007**, *76*, 1535-1541.
40. Liscano, Y.; Salamanca, C. H.; Vargas, L.; Cantor, S.; Laverde-Rojas, V.; Oñate-Garzón, J. Increases in hydrophilicity and charge on the polar face of alyteserin 1c helix change its selectivity towards Gram-positive bacteria. *Antibiotics (Basel).* **2019**, *8*, 238.
41. Palermo, E. F.; Lienkamp, K.; Gillies, E. R.; Ragogna, P. J. Antibacterial activity of polymers: discussions on the nature of amphiphilic balance. *Angew Chem Int Ed Engl.* **2019**, *58*, 3690-3693.
42. Judzewitsch, P. R.; Nguyen, T. K.; Shanmugam, S.; Wong, E. H. H.; Boyer, C. Towards sequence-controlled antimicrobial polymers: effect of polymer block order on antimicrobial activity. *Angew Chem Int Ed Engl.* **2018**, *57*, 4559-4564.
43. Lam, S. J.; O'Brien-Simpson, N. M.; Pantarat, N.; Sulistio, A.; Wong, E. H.; Chen, Y. Y.; Lenzo, J. C.; Holden, J. A.; Blencowe, A.; Reynolds, E. C.; Qiao, G. G. Combating multidrug-resistant Gram-negative bacteria with structurally nanoengineered antimicrobial peptide polymers. *Nat Microbiol.* **2016**, *1*, 16162.
44. Osmanoğlu, Y. E.; Sütçü, K. EPR studies of the free radicals generated in gamma irradiated amino acid derivatives. *J Mol Struct.* **2017**, *1145*, 240-243.
45. Duliu, O. G.; Bercu, V. Chapter 2 - ESr investigation of the free radicals in irradiated foods. In *Electron spin resonance in food science*, Shukla, A. K., ed. Academic Press: 2017; pp 17-32.
46. Atrous, H.; Benbettaieb, N.; Hosni, F.; Danthine, S.; Blecker, C.; Attia, H.; Ghorbel, D. Effect of γ-radiation on free radicals formation, structural changes and functional properties of wheat starch. *Int J Biol Macromol.* **2015**, *80*, 64-76.
47. Liu, W.; Wang, M.; Xing, Z.; Wu, G. The free radical species in polyacrylonitrile fibers induced by γ-radiation and their decay behaviors. *Radiat Phys Chem.* **2012**, *81*, 835-839.
48. Zhao, Y.; Wang, M.; Tang, Z.; Wu, G. ESR study of free radicals in UHMW-PE fiber irradiated by gamma rays. *Radiat Phys Chem.* **2010**, *79*, 429-433.

Received: January 5, 2023
Revised: Febraury 17, 2023
Accepted: March 9, 2023
Available online: March 28, 2023

Additional file 1 Preparation and characterisation of the N-carboxyanhydrides and antimicrobial peptides

Preparation and characterisation of the N-carboxyanhydrides

Synthesis of Nε-tert-butyloxycarbonyl-L-lysine N-carboxyanhydride (Boc-L-Lys-NCA): Boc-L-Lys (10.0 g, 40.6 mmol) was suspended in 180 mL of tetrahydrofuran (THF) in a round-bottomed flask at 50°C, followed by addition of a solution of triphosgene (4.4 g, 14.9 mmol) in THF (20 mL). The reaction media became clarified around 10 minutes after the complete addition of triphosgene. Then the reaction mixture was cooled to room temperature, and the solvent was removed by rotary evaporation to yield a crude product, which was re-crystallised three times using ethyl acetate and hexane to yield a white powder (5.1 g, 46.1% yield). ^{1}H nuclear magnetic resonance spectroscopy (400 MHz, dimethyl sulfoxide-d_6) δ (ppm): 9.06 (s, ^{1}H-1.00, -CON***H***CH-), 6.77 (t, ^{1}H-1.00, -CH_2N***H***COO-), 4.46–4.36 (m, ^{1}H-1.00, -NHC***H***CH_2-), 2.90 (q, ^{2}H-2.05, -CHC***H***$_2$$CH_2$-), 1.81–1.58 (m, ^{2}H-2.05, -C***H***$_2$NHCOO-), 1.39–1.22 (m, ^{13}H-13.45, -$CH_2CH_2CH_2$NHCOOC(***CH***$_3$)$_3$).[1]

Synthesis of D-phenylalanine (Phe) NCA: A solution of triphosgene (6.6 g, 22.2 mmol) in THF (20 mL) was added into 10.0 g of D-phe (60.5 mmol) that was pre-dispersed in THF (180 mL) in a round-bottomed flask at 50°C. The mixture was stirred vigorously until the solution became clear (approximately 60 min). A white powdery product (6.2 g, 53.6% yield) was obtained after three re-crystallisations from ethyl acetate/hexane. 1H nuclear magnetic resonance spectroscopy (400 MHz, chloroform-*d* ($CDCl_3$)) δ (ppm): 7.43–7.03 (m, ^{5}H-5.47, ***ArH***CH_2-), 6.38 (s, ^{1}H-1.00, -CON***H***CH-), 4.53 (dd, ^{1}H-1.10, -NHC***H***CH_2-), 3.25 (dd, ^{1}H-1.10, ArC***H***$_2$CH-), 3.01 (dd, 1H-1.10, ArC***H***$_2$CH-).[1]

Synthesis of D, L-valine (Val) NCA: A solution of triphosgene (10.1 g, 34.1 mmol) in THF (30 mL) was mixed with 170 mL of D, L-Val solution (10.0 g, 85.4 mmol, dissolved in THF) in a round-bottomed flask. The mixture was heated to 50°C and stirred vigorously for 60 minutes. Then the solvent was removed by rotary evaporation, and D, L-Val-NCA (6.2 g, 53.6% yield) was obtained after three re-crystallisations from ethyl acetate/hexane. 1H nuclear magnetic resonance spectroscopy (400 MHz, dimethyl sulfoxide-d6): δ 9.10 (s, ^{1}H-0.94, -N***H***-), 4.34 (d, ^{1}H-0.95, -NHC***H***(CO)CH-), 2.17–1.88 (m, ^{1}H-1.00, $(CH_3)_2$C***H***-), 0.90 (dd, ^{6}H-6.06, $(CH_3)_2$C***H***-) (**Figure 1**).[1]

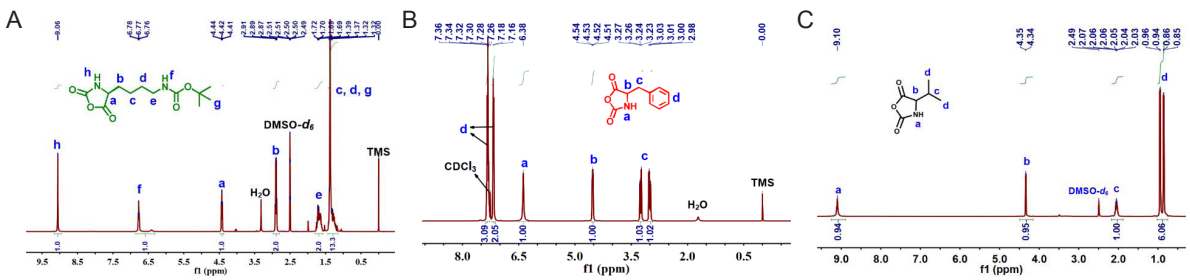

Figure 1. ^{1}H nuclear magnetic resonance spectroscopy of Nε-tert-butyloxycarbonyl-L-lysine N-carboxyanhydride (Boc-L-Lys-NCA) (A), D-phenylalanine N-carboxyanhydride (D-Phe-NCA) (B) and D, L-valine N-carboxyanhydride (D, L-Val-NCA) (C).

Preparation and characterisation of the antimicrobial peptides

The specific synthetic steps of the different antimicrobial peptides (AMPs) have been published in our previous work.[1] G2-PAMAM and n-hexylamine were chosen as initiators for the synthesis of star-shaped and linear AMPs, respectively. Put simply, 2 mmol of the appropriate monomers (Boc-L-Lys-NCA, D-Phe-NCA or D, L-Val-NCA) were dissolved in 10 mL of dry THF solution ([M]0 = 0.2 M), followed by adding an initiator/*N*, *N*-dimethylformamide solution containing a primary amine content of 0.067 mmol (feeding ratio: monomer/initiator = 30). Then, the reaction solution was stirred at room temperature. Meanwhile, drops of reaction solution were taken out for analysis by Fourier transform infrared spectroscopy at different time points. The reaction was completed when the characteristic peaks of the monomers at 1852 cm^{-1} and 1780 cm^{-1} disappeared. Then, 100 μL of the solution was taken out for analysis by gel permeation chromatography. The products were collected by precipitating the remaining solution into cold ether, followed by centrifugation and vacuum drying. Subsequently, excess trifluoroacetic acid was added to the above products and stirred for another 12 hours for the deprotection of BOC groups. The mixture was transferred to dialysis bags with a molecular weight cut-off of 3500 g/mol and 8000–12,000 g/mol for the linear and star-shaped AMPs, respectively. After dialyzing against ultra-pure water for three days, the AMPs were obtained by lyophilisation. The molecular parameters of all products were confirmed by 1H nuclear magnetic resonance spectroscopy (**Figure 2**).[2]

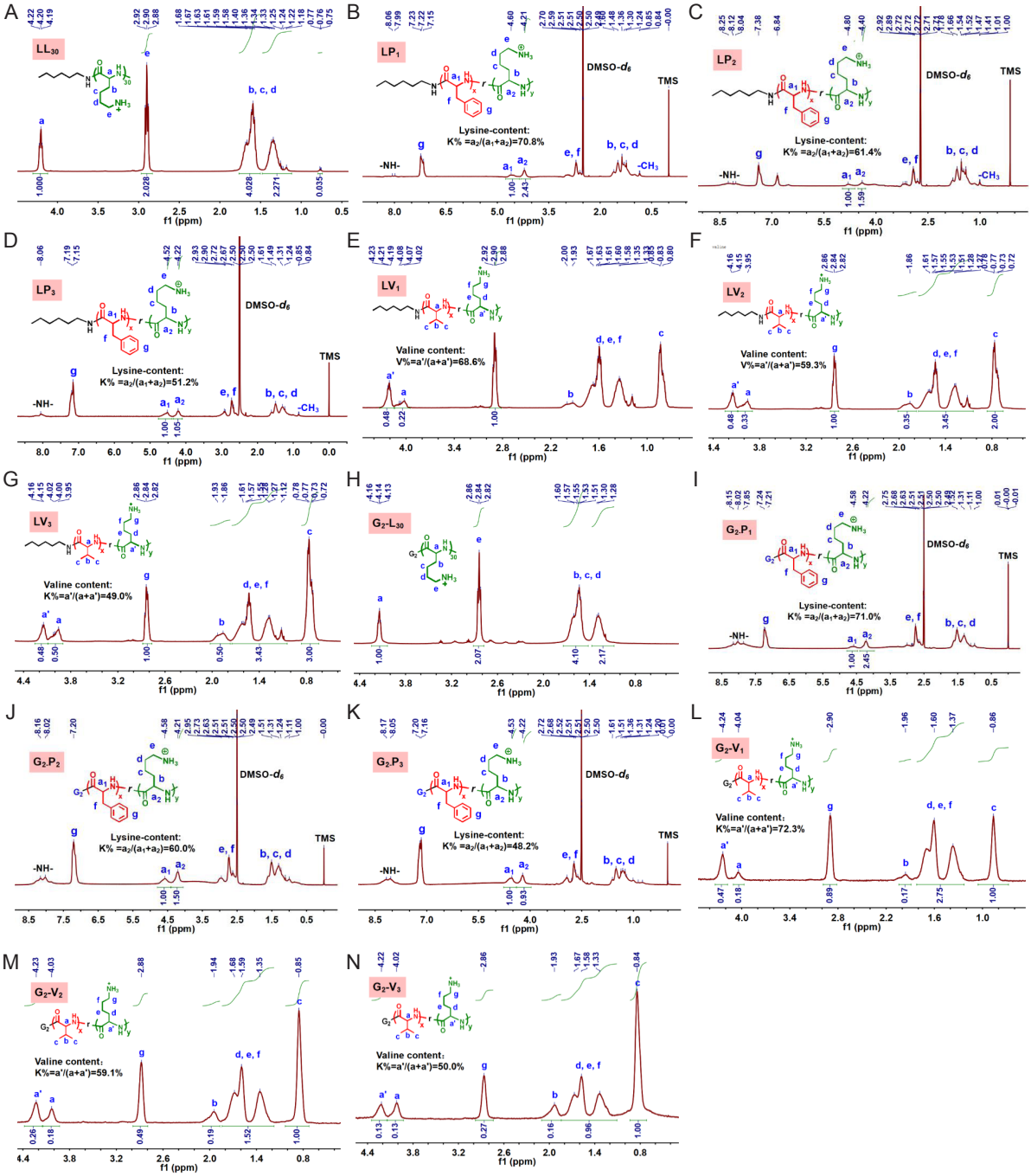

Figure 2. ^{1}H nuclear magnetic resonance spectroscopy of LL_{30} (A), LP_1 (B), LP_2 (C), LP_3 (D), LV_1 (E), LV_2 (F), LV_3 (G), G_2-L_{30} (H), G_2-P_1 (I), G_2-P_2 (J), G_2-P_3 (K), G_2-L_{30} (L), G_2-L_{30} (M) and G_2-L_{30} (N).

1. Wang, X.; Yang, F.; Yang, H.; Zhang, X.; Tang, H.; Luan, S. Preparation of antibacterial polypeptides with different topologies and their antibacterial properties. *Biomater Sci.* **2022**, *10*, 834-845.

2. Raza, S.; Iqbal, Y.; Ullah, I.; Mubarak, M. S.; Hameed, M. U.; Raza, M. Effects of gamma irradiation on the physico-chemical and biological properties of levofloxacin. *Pak J Pharm Sci.* **2018**, *31*, 181-186.